JCI insight

RESEARCH ARTICLE

Red blood cell β-adrenergic receptors contribute to diet-induced energy expenditure by increasing O_2 supply

Eun Ran Kim,[1] Shengjie Fan,[1,2] Dmitry Akhmedov,[3] Kaiqi Sun,[4] Hoyong Lim,[1] William O'Brien,[4] Yuanzhong Xu,[1] Leandra R. Mangieri,[1,5] Yaming Zhu,[1] Cheng-Chi Lee,[4] Yeonseok Chung,[1] Yang Xia,[4] Yong Xu,[6] Feng Li,[7] Kai Sun,[1] Rebecca Berdeaux,[1,3] and Qingchun Tong[1,5]

[1]Brown Foundation Institute of Molecular Medicine and University of Texas McGovern Medical School, Houston, Texas, USA. [2]School of Pharmacy, Shanghai University of Chinese Traditional Medicine, Shanghai, China. [3]Department of Integrative Biology and Pharmacology, Graduate Program in Cell and Regulatory Biology, Graduate School of Biomedical Sciences, [4]Department of Biochemistry and Molecular Biology, Graduate Program in Biochemistry, and [5]Department of Neurobiology and Anatomy, Graduate Program in Neuroscience, Graduate School of Biological Sciences, University of Texas McGovern Medical School, Houston, Texas, USA. [6]Children's Nutrition Research Center, Department of Pediatrics, and [7]Department of Molecular and Cellular Biology, Baylor College of Medicine, Houston, Texas, USA.

Diet-induced obesity (DIO) represents the major cause for the current obesity epidemic, but the mechanism underlying DIO is unclear. β-Adrenergic receptors (β-ARs) play a major role in sympathetic nervous system–mediated (SNS-mediated) diet-induced energy expenditure (EE). Rbc express abundant β-ARs; however, a potential role for rbc in DIO remains untested. Here, we demonstrated that high-fat, high-caloric diet (HFD) feeding increased both EE and blood O_2 content, and the HFD-induced increases in blood O_2 level and in body weight gain were negatively correlated. Deficiency of β-ARs in rbc reduced glycolysis and ATP levels, diminished HFD-induced increases in both blood O_2 content and EE, and resulted in DIO. Importantly, specific activation of cAMP signaling in rbc promoted HFD-induced EE and reduced HFD-induced tissue hypoxia independent of obesity. Both HFD and pharmacological activation cAMP signaling in rbc led to increased glycolysis and ATP levels. These results identify a previously unknown role for rbc β-ARs in mediating the SNS action on HFD-induced EE by increasing O_2 supply, and they demonstrate that HFD-induced EE is limited by blood O_2 availability and can be augenmented by increased O_2 supply.

Introduction

The current obesity epidemic is due to a combination of genetic susceptibility and availability of high-fat, high-caloric diet (HFD) (1–3). The brain coordinates physiological processes systemically to reduce energy intake and increase energy expenditure (EE) in response to HFD feeding to maintain body weight homeostasis (1). The alarming rate of obesity development during recent decades correlates with rapid economic development and availability of HFD (3), suggesting that the defective response to HFD feeding is one of the major reasons for the obesity epidemic. Despite extensive research, the underlying mechanism responsible for the susceptibility to diet-induced obesity (DIO) is not yet clear.

As a major determinant of body weight, EE largely depends on mitochondrial oxidative metabolism and thermogenesis (4), in which nutrient substrates and O_2 are required. While nutrient flux and metabolism in key metabolic tissues have been major research focuses (1, 5, 6), a potential direct contribution of defective O_2 supply to obesity development has largely been neglected. In this regard, a subtle change in O_2 supply may affect mitochondrial metabolism, which may ultimately lead to a considerable alteration in body weight (7). Although changes in blood flow and tissue O_2 availability have been studied in the context of obesity, most studies focus on these changes as a consequece of obesity (8, 9). Whether defective blood O_2 supply directly contributes to HFD-induced obesity is unknown.

HFD feeding acutely induces EE in both rodents and humans (10). The sympathetic nervous system (SNS) plays an important role in mediating the brain action on EE regulation (11). Activation of the SNS mobilizes fat from white adipose tissues and increases the activity of brown adipose tissues, thereby

Conflict of interest: The authors have declared that no conflict of interest exists.

Submitted: February 10, 2017
Accepted: June 1, 2017
Published: July 20, 2017

Reference information:
JCI Insight. 2017;2(14):e93367.
https://doi.org/10.1172/jci.insight.93367.

increasing EE (11, 12). Mice lacking all β-adrenergic receptors (β-ARs), also known as β-less mice, exhibit great susceptibility to DIO associated with diminished responses in diet-induced EE but with no changes in food intake (13), demonstrating a major role for β-ARs in mediating the SNS-mediated diet-induced EE. However, given the ubiquitous expression of β-ARs, it remains unclear which specific tissue(s) contribute to β-AR–mediated diet-induced EE and can therefore be targeted for therapeutics against DIO.

HFD-induced obesity is associated with tissue hypoxia (14–18), suggesting a state of insufficient O_2 supply. However, despite evidence showing that obesity is associated with tissue hypoxia (8, 19, 20), it is unknown whether tissue hypoxia occurs prior to and therefore contributes to DIO. However, it is conceivable that insufficient tissue O_2 supply may cause insufficient diet-induced EE and contribute to DIO. Rbc express abundant β-ARs (21) and therefore may play an important role in mediating SNS action induced by HFD feeding. Given the major role of rbc in blood O_2 supply, we hypothesize that rbc respond to HFD-induced SNS activation by providing sufficient blood O_2 availability to meet the increased demand for O_2 for HFD-induced EE. Here, we demonstrated that the β-AR–cAMP signaling pathway in rbc were both required and sufficient to mediate HFD-induced EE and blood O_2 content, and we identified a previously unappreciated role for rbc O_2 supply in HFD-induced EE and DIO.

Results

Correlation between body weight and blood O_2 content. We used an Avoximeter (Avox 1000, ITC International) to measure O_2 content, saturation (percent of oxygenated hemoglobin [Hb]) and total Hb. To achieve repeatable measurements of blood O_2 levels from conscious, nonstressed animals, we used tail blood — a mixture of venous and arterial blood — since blood O_2 content responds rapidly to anesthetics and other stressful conditions (22). We found that the O_2 content in tail blood was within a range of 8–20 ml/dl, and the O_2 saturation was within a range of 40%–80%. As expected, EE was higher during the dark period than the light period (Supplemental Figure 1A; supplemental material available online with this article; https://doi.org/10.1172/jci.insight.93367DS1). Interestingly, the blood O_2 level in the dark period (zeitgeber time [ZT] 12–ZT13) was higher (Supplemental Figure 1, B and C), compared with those in the light period (ZT5–ZT6). Total Hb was higher in the light period than the dark period (Supplemental Figure 1D), an observation that is consistent with a previous report (23). These results show that blood O_2 levels correlated diurnal changes in EE.

HFD reversibly increased EE and blood O_2 content. Mice within the C57BL/6J (C57) strain, despite the same genetic background, exhibit differential susceptibility to DIO (24). Interestingly, blood O_2 content and saturation of these chow-fed mice were negatively correlated with their body weight (Figure 1A and Supplemental Figure 1E) but not with either daily food intake (Supplemental Figure 1F) or Hb (data not shown). To examine the effect of HFD feeding, we measured EE, first on chow and then switched to HFD, each for 3 days (Figure 1B). EE was significantly increased in HFD compared with chow (Supplemental Figure 1, G and H). Blood O_2 content was also increased (Figure 1C). Interestingly, in response to HFD, rbc isolated from these mice showed an increase in both cAMP (Supplemental Figure 1I) and ATP (Supplemental Figure 1J) as well as a significant reduction in the ratio of glucose-6-phosphate(fructose-6-phophate)/lactate (Supplemental Figure 1K), an indicator of increased glucose metabolism. These changes are consistent with the notion that HFD feeding increases the SNS activity, leading to β-AR activation in rbc, thereby promoting glucose metabolism and increasing ATP levels. HFD failed to cause a change in 2,3-diphosphoglycerate (2,3-DPG, Supplemental Figure 1L) or P50 (Supplemental Figure 1M), known indicators for O_2-Hb affinity, suggesting that the increased O_2 content is unlikely due to a change in O_2-Hb affinity.

To examine whether the effect of HFD feeding on blood O_2 content persists, C57 male mice were fed HFD from 8–18 weeks of age and then randomly divided into two groups: one continuously fed HFD and the other switched back to chow diet. We measured EE during the diet switch (Figure 1D). While no difference in EE was noticed before the diet switch, mice that were switched to chow showed significantly lower EE compared with those continuously fed HFD (Figure 1E). Interestingly, blood O_2 content was also reduced in mice that were switched to chow (Figure 1F). These results indicate that the effect of HFD feeding on EE and blood O_2 content is stable up to at least 10 weeks of HFD feeding but reverts when the animals are switched back to a normal chow diet. We monitored changes in body weight and O_2 content in C57 mice before and after an 8-week HFD feeding regimen (Figure 1G) and found a significantly negative correlation between HFD-induced body weight gain and HFD-induced increases in O_2 content (Figure 1H). These results strongly support the notion that increased blood O_2 availability contributes to HFD-induced EE.

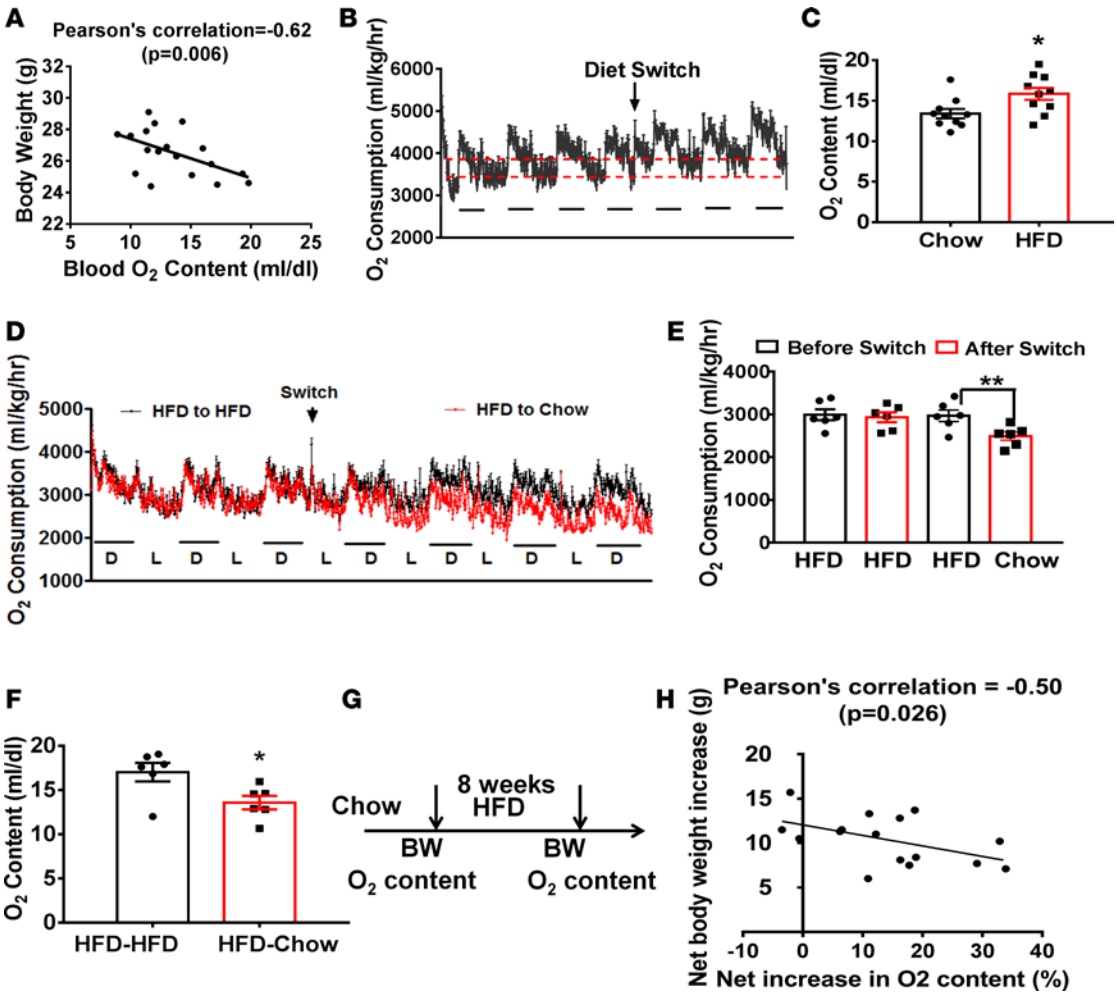

Figure 1. HFD feeding reversibly increases energy expenditure and blood O_2 content. (**A**) Correlation between blood O_2 content and body weight measured in a cohort of C57 male mice (9–10 weeks old, n = 18). (**B** and **C**) Energy expenditure (**B**) and blood O_2 content in a cohort of C57 male mice during chow high-fat, high-sucrose diet (HFD) transition (n = 10/group). (**D–F**) O_2 consumption measured a cohort of C57 male mice first fed HFD from 8–18 weeks of age. Then, half of the mice were switched to chow and the other were kept on HFD. O_2 consumption was measured during diet switch (**D**), and comparisons in O_2 consumption (**E**) and O_2 contents (**F**) 3 days before and 1 week after diet switch (n = 6/group) were measured. (**G** and **H**) A diagram showing the procedure for O_2 content and body weight measurements in a cohort of C57 males reared on chow (9–10 weeks old, n = 17) and then fed HFD for 8 weeks (**G**), and correlation between net increases in body weight and those in blood O_2 content by Parson's correlation tests (**H**). L, light period; D, dark period. Dashed lines in **B** and **G** indicate dark periods. All data are presented as mean ± SEM; $^*P < 0.05$, $^{**}P < 0.01$ by paired student's t tests (**C**), unpaired student's t tests (**F**), or 2 way ANOVA tests with Tukey post-hoc analysis (**E**).

To examine whether similar responses to HFD also exist in FVB mice, we measured body weight and O_2 responses to HFD in these mice. We found a significant negative correlation between body weight and O_2 content (Supplemental Figure 2A) and, in response to HFD, significant increases in rbc of cAMP (Supplemental Figure 2B), ATP (Supplemental Figure 2C), and glucose-6-p(fructose-6-p)/lactate (Supplemental Figure 2D) in FVB mice. In addition, there was also a significant negative correlation between net increases in O_2 content and net increases in body weight in response to HFD (Supplemental Figure 2E). These data suggest that the HFD effect on O_2 content and blood cAMP, glucose metabolism, and the potential impact on body weight changes is not specific to C57 mice, but rather holds true across animal strains.

Activation of β-ARs increased both EE and O_2 content. Activation of β-ARs by the nonselective β-AR agonist, isoproterenol (Iso), increased O_2 consumption in WT but not β-less mice, both on the FVB background (Figure 2A). Iso also increased blood O_2 content (Figure 2B) and saturation (Figure 2C) in WT mice, but it had no effects on either in β-less mice (Figure 2, B and C). The increases were not due to a change in the Hb amount because Iso had no effects on Hb levels in either group (Supplemental Figure 3A). The increased O_2 content in WT mice was not due to less O_2 usage because O_2 consumption in these mice was increased rather than reduced (Figure 2A), suggesting an increased O_2 loading to blood. Notably, β-less mice had

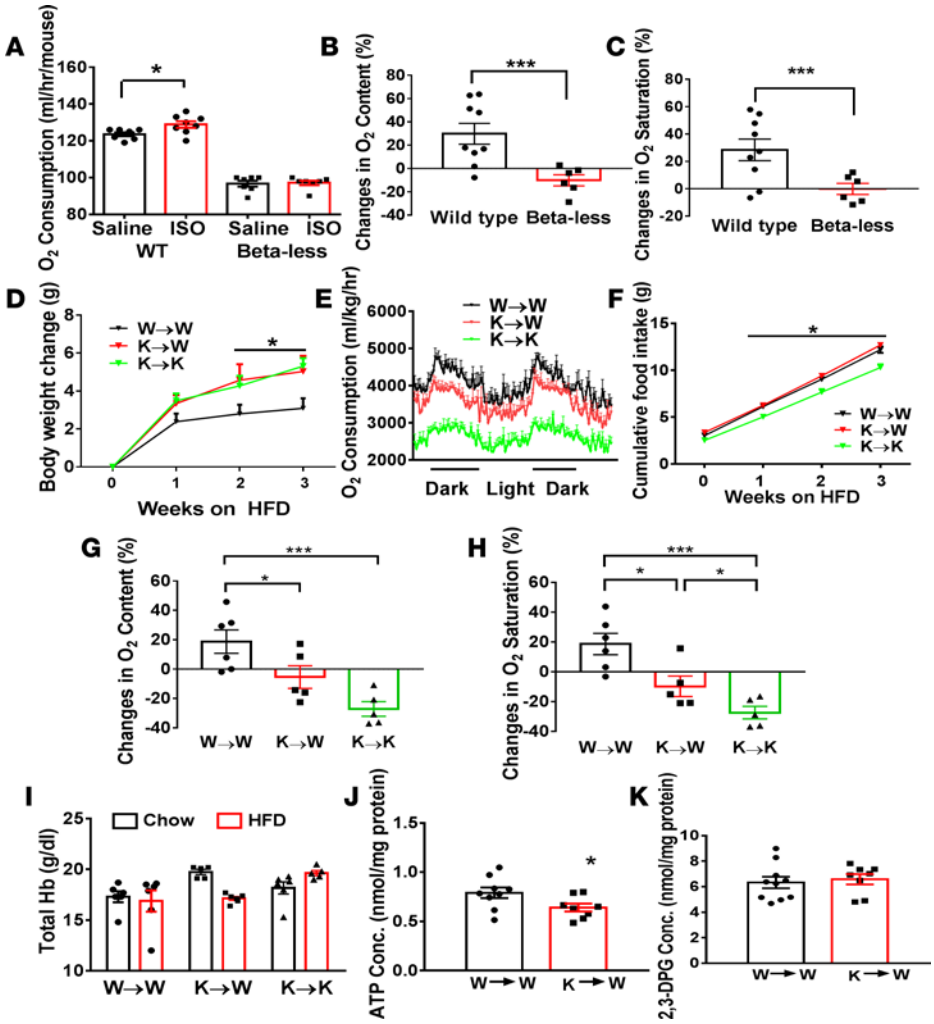

Figure 2. Rbc β-ARs are required for HFD-induced EE and increases in O_2 content. Male β-less mice (i.e., lacking all 3 β-adrenergic receptors) on the FVB background and WT FVB mice with similar ages were used for this study. (**A–C**) Eight- to 10-week-old control and β-less male mice (n = 6–9/group) received s.c. injection of saline or isopreteneronol (Iso) (1 mg/kg, bw), and O_2 consumption (**A**), changes in blood O_2 content (**B**), and changes in O_2 saturation (**C**) were measured within 3.5 hrs of drug administration. (**D–K**) BM transplantation (BMT) was performed by injecting BM from β-less mice to lethal dose–irradiated controls (K→W mice) or to β-less mice (K→K) or by injecting BM from controls to lethal dose–irradiated controls (W→W mice). All mice used were young males (12–16 weeks of age, n = 5–6/group) and measured for weekly body weight (**D**), O_2 consumption (**E**), food intake (**F**), changes in blood O_2 contents (**G**), changes in O_2 saturation (**H**), and total Hb (**I**) 3 days before and 5 weeks after HFD. (**J** and **K**) Measurements of rbc ATP (**J**) and 2,3-DPG (**K**) in the indicated 3 groups of mice 5 weeks after HFD (n = 8–10/group). The data presented in **J** and **K** were samples combined from 2 BMT experiments. All data are presented as mean ± SEM; $^*P < 0.05$, $^{***}P < 0.005$ by 2-way ANOVA tests in **A** and **D–F**; 1-way ANOVA tests in **G** and **H**; and unpaired Student's t tests in **B** and **C** and **J** and **K**.

much higher rbc numbers (Supplemental Figure 3B) and mean corpuscular Hb levels (Supplemental Figure 3C). Rbc from β-less mice had significantly lower cAMP (Supplemental Figure 3D), consistent with loss of β-AR function. In addition, they had an increased ratio of glucose-6-phosphate(fructose-6-phosphate)/lactate (Supplemental Figure 3E), indicating reduced glucose metabolism. There was no obvious difference in 2,3-DPG (Supplemental Figure 3F) or P50 (Supplemental Figure 3G) between β-less mice and controls, suggesting no major changes in Hb-O_2 affinity in β-less mice. Given the known role of β-ARs in early tissue development and vasodilation (13, 25), the increased rbc number and Hb level may reflect a compensatory response to reduced O_2 availability and hypoxia in metabolic tissues of β-less mice.

Rbc β-ARs are required for HFD-induced EE and increases in O_2 content. To examine the role of β-ARs in rbc, we performed BM transplantation (BMT) to replace BM of control mice with that of β-less mice (K→W mice). These mice were used as a model of selective β-AR KO in hematopoietic cells. BMT between controls (W→W) and between β-less mice (K→K) was used as a control. cAMP was significantly reduced in rbc isolated from the K→W group, compared with the W→W group, and were comparable in the K→K group (Supplemental Figure 4A), suggesting successful BMT and the importance of rbc β-ARs in the regulation of rbc intracellular cAMP levels.

β-Less mice develop massive obesity on HFD but exhibit normal body weight on a chow diet (13). Therefore, we focused on body weight responses to HFD feeding. Four weeks after BMT (to allow full reconstitution of the hematopoietic system with BM-derived cells), all mice were switched to HFD. Within 3 weeks on HFD, compared with W→W mice, K→W mice significantly increased their body weight to a level comparable with K→K mice (Figure 2D). The increased body weight was associated with increased fat accumulation but with no changes in lean mass (Supplemental Figure 4, B and C), indicating obesity development. As

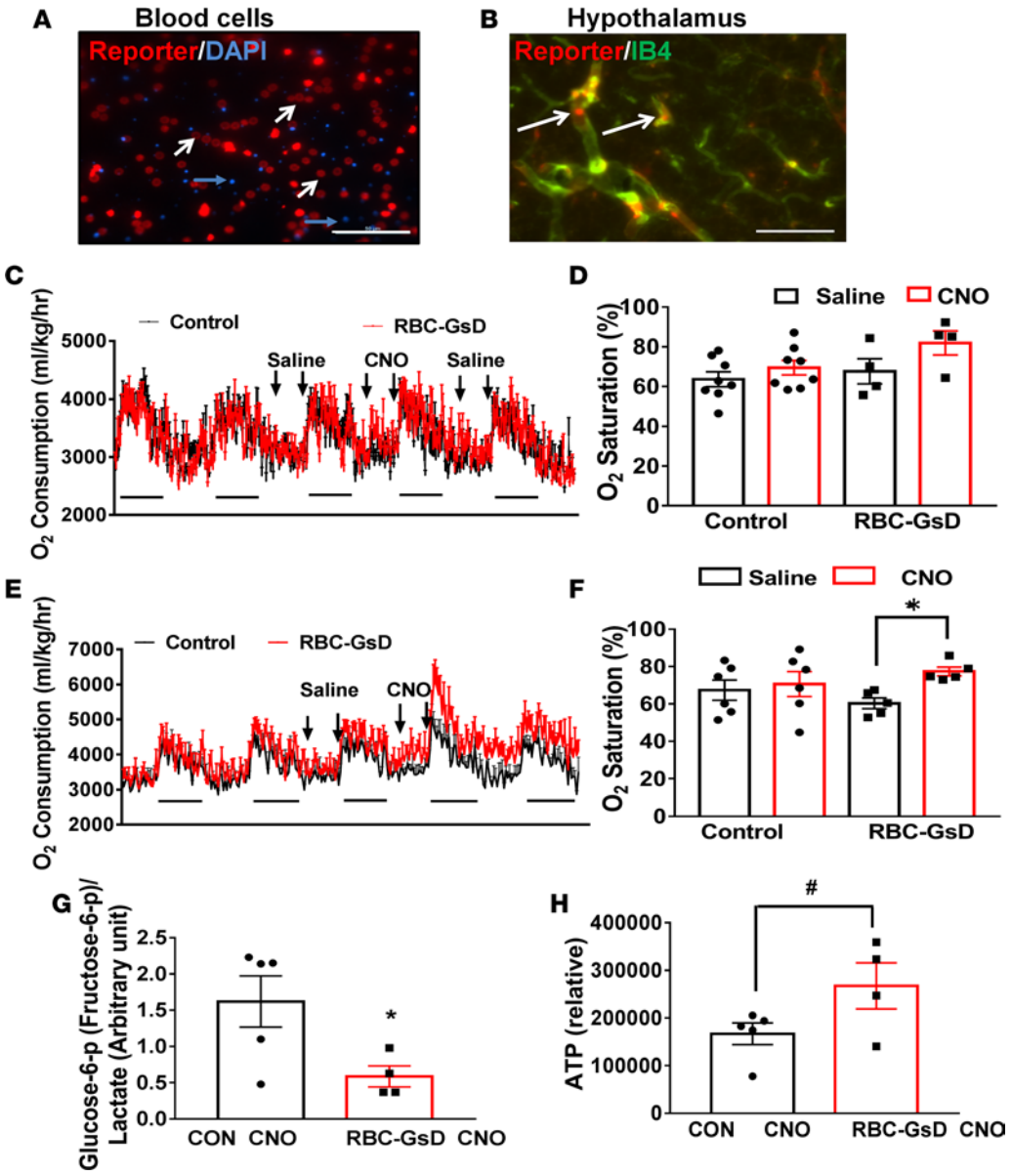

Figure 3. Activation of Gs signaling in rbc increases HFD-induced EE and blood O_2 content. (**A** and **B**) EpoR-Cre expression pattern shown by tdTomato (red fluorescence) in EpoR-Cre Ai9 reporter mice in blood cells (**A**) and brain tissues (**B**). Note that in **A**, all reporter-positive Cre-expressing blood cells (white arrows) were negative for DAPI (blue arrows), a marker for nuclei, suggesting rbc; in **B**, the Cre-expressing structures (white arrows) in the brain were confined in blood vessels as marked by IB4 expression (green), suggesting rbc trapped in blood vessels. (**C** and **D**) Acute effects of CNO injection in mice on chow. Rbc-GsD mice and littermate controls (8–10 weeks of age, males, n = 4–8/group) were i.p. injected with saline and CNO (1 mg/kg, bw) as indicated and were measured for O_2 consumption (**C**) and O_2 saturation (**D**). (**E** and **F**) Acute effects of CNO injections in mice on HFD. Rbc-Gs mice and littermate controls (8–10 weeks of age, males, n = 5–6) fed HFD and were measured for O_2 consumption (**E**) and O_2 saturation (**F**). (**G** and **H**) Levels of glucose-6-p(fructose-6-p)/lactate (**G**) and ATP (**H**) in rbc 50 min after receiving i.p. CNO (1 mg/kg, bw) from a cohort of control and RBD-GsD mice fed HFD for 2 weeks (n = 4–5/group). Rbc-GsD, EpoR-Cre::Rosa26-LSL-Gs-DREADD. Scale bar: 50 μM. Dashed lines in **E** indicates dark periods. All data presented as mean ± SEM; $^*P < 0.05$, $^{\#}P$ = 0.06 by unpaired Student's t tests.

expected, like β-less mice, K→K mice showed greatly reduced EE (Figure 2E). Interestingly, compared with W→W mice, K→W mice showed markedly reduced EE when the data were normalized by body weight (Figure 2E) or analyzed per animal (Supplemental Figure 4D). Surprisingly, unlike previous results showing β-less mice had a normal feeding level, K→K mice had a much reduced feeding level on HFD (Figure 2F). The reduced food intake in K→K mice was not due to a secondary effect of BMT, since naive β-less mice also exhibited reduced feeding associated with much reduced EE and mild obesity on HFD (data not shown), similar to K→K mice, as opposed to massive DIO demonstrated previously (13). The reason underlying this

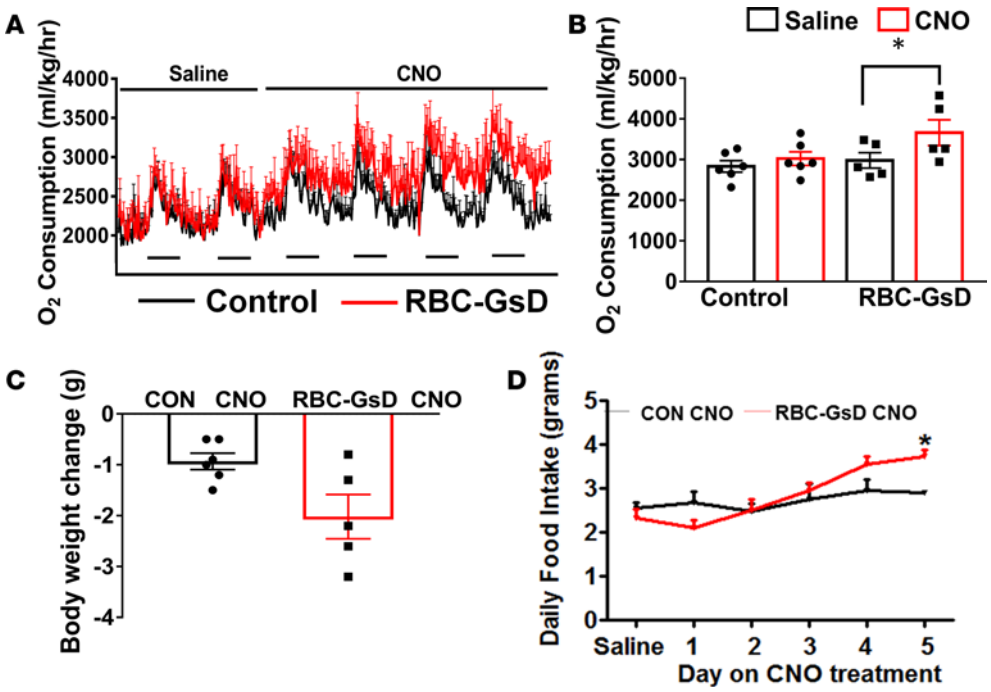

Figure 4. Activation of rbc-Gs signaling resulted in increased HFD-induced energy expenditure. Rbc-GsD mice and littermate controls (8–10 weeks of age, males, n = 5–6/group) were fed HFD for 10 weeks and received daily i.p. injections of CNO (1 mg/kg, bw, 10:00 and 17:00) for 2 weeks while continuously fed HFD. (**A**) O_2 consumption measured for the first 4 days on CNO administration. (**B** and **C**) Responses in O_2 consumption to CNO (**B**), changes in body weight (**C**), and daily feeding (**D**) in these mice were measured. Rbc-GsD, EpoR-Cre::Rosa26-LSL-Gs-DREADD. Dashed lines in **A** indicate dark periods. All data are presented as mean ± SEM; *P < 0.05 by unpaired Student's t tests (**D**) or 2-way ANOVA with Tukey post-hoc analysis (**B**).

difference is unknown but might be due to different genetic backgrounds. The β-less mice previously reported were on a mixed C57 and 129 background, while the current animals were derived from back-crossing to generate the mice on a pure FVB background. Nonetheless, K→K mice had no difference in locomotor activity (Supplemental Figure 4E) or respiration exchange ratio (RER) (Supplemental Figure 4F) compared with W→W mice. Thus, DIO in K→K mice was a result of combined effects of reduced feeding and EE, while that in K→W mice was solely due to reduced EE. These results suggest that rbc account for an important part of HFD-induced EE mediated by β-ARs.

To examine whether loss of β-ARs in rbc, the major component of BM-derived cells, were responsible for the blunted diet-induced EE in K→W mice, we measured blood O_2 content before and after HFD feeding. HFD induced a significant increase in both blood O_2 content (Figure 2G) and saturation in W→W mice, but it failed to do so in K→W mice (Figure 2H), confirming that β-ARs in rbc are required for HFD-induced increases in O_2 levels. These changes in O_2 content were not due to a change in total Hb amounts (Figure 2I). Rbc from K→W mice showed lower ATP levels (Figure 2J) but no difference in 2,3-DPG levels (Figure 2K) compared with W→W mice, suggesting that changes in blood O_2 content by deficient rbc β-ARs are not due to a change in Hb-O_2 affinity, but rather are associated with reduced ATP levels. These results demonstrate that β-ARs in rbc are required for the brain to promote diet-induced EE through increasing blood O_2 content via SNS-mediated activation of rbc.

Activation of cAMP signaling in rbc increases HFD-induced EE and blood O_2 content. To test the function of β-AR signaling in rbc, we generated mice with inducible rbc-specific activation of Gs-cAMP signaling, known to be one of the major downstream signals of β-ARs. We crossed a new strain of ROSA26-LSL-Gs-DREADD mice, which allow Cre recombinase–sensitive expression of a Gs-selective designer receptors exclusively activated by designer drugs (DREADD), with erythropoietin receptor–Cre (EpoR-Cre) mice to generate EpoR-Cre::ROSA26-LSL-Gs-DREADD (rbc-GsD) mice. DREADDs are mutated muscarinic GPCRs with selectivity for individual G protein effector pathways (Gs, Gi, or Gq) and only respond to the otherwise inert ligand clozapine *N*-oxide (CNO) (26). ROSA26-LSL-Gs-DREADD animals enable temporal control of cAMP signaling in selective cell types using cell type–specific Cre drivers (27). EpoR-Cre

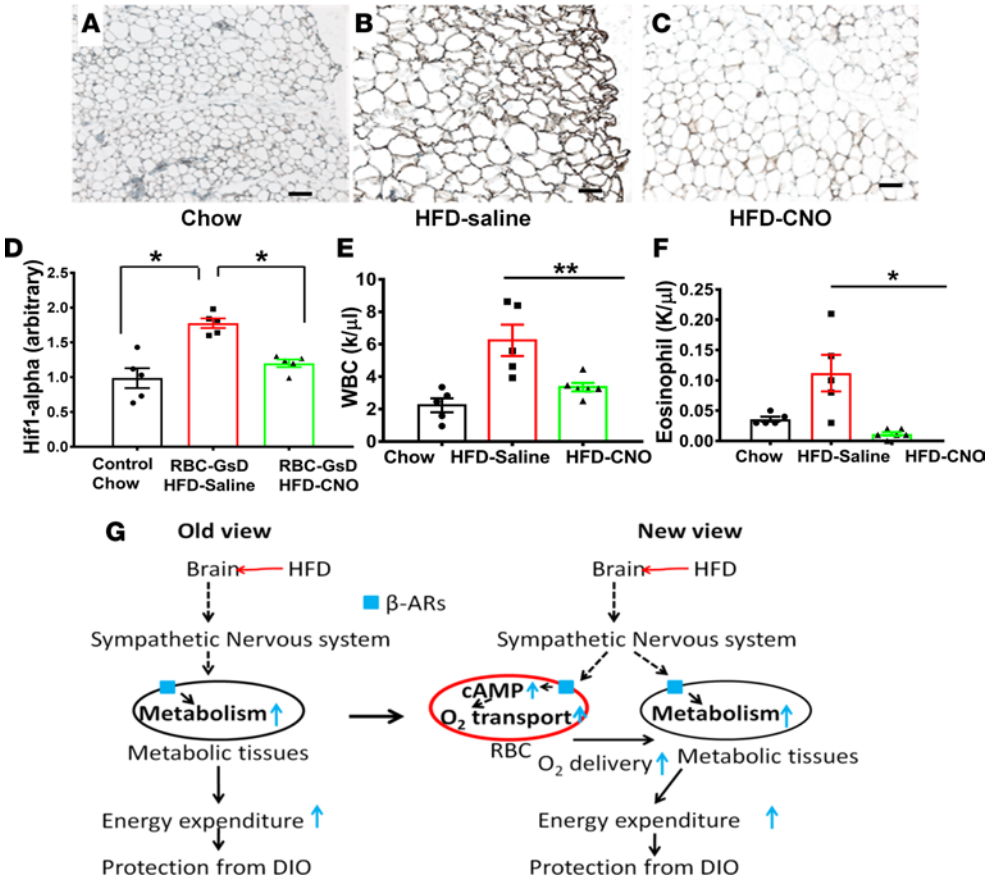

Figure 5. Activation of rbc-Gs signaling reduced tissue hypoxia induced by HFD. Rbc-GsD mice and littermate controls (8–10 weeks of age, males, n = 5–6/group) were fed HFD for 10 weeks and received daily i.p. injections of CNO (1 mg/kg, bw, 10:00 and 17:00) for 2 weeks while continuously fed HFD. (**A–C**) Hypoxia was measured in adipose tissues of chow-fed controls (**A**), HFD-fed rbc-GsD mice treated with saline (**B**), and HFD-fed rbc-GsD mice treated with CNO (**C**). (**D**) Expression levels of *Hif1α* mRNA expression by qPCR from adipose tissues of the indicated genotypes. (**E** and **F**) Results from a blood count of white blood cells (**E**) and eosinophil (**F**) after HFD. (**G**) A diagram depicting a change from an old view to a new view on physiological pathways engaged in responses to HFD, with emphasis on the role of rbc. Activation of SNS by HFD leads to a coordinated activation of metabolic tissues and rbc, which then meet the higher demand for more O_2 in metabolic tissues to promote sufficient diet-induced energy expenditure for normal body weight homeostasis. Rbc-GsD, EpoR-Cre::Rosa26-LSL-Gs-DREADD. Scale bars: 100 μm. All data are presented as mean ± SEM; $^*P < 0.05$, $^{**}P < 0.01$ by 1-way ANOVA.

mice were used to achieve rbc-specific expression of Cre (28, 29). To verify an EpoR-Cre expression pattern, we crossed EpoR-Cre mice with ROSA26-LSL-tdTomato (Ai9) Cre reporter mice (30). The expression of tdTomato reporter was detected in $DAPI^-$ cells, but not in $DAPI^+$ cells, in a whole blood preparation (Figure 3A), suggesting a specific Cre-expression pattern in enucleated rbc. We also detected EpoR-Cre–driven tdTomato reporter expression in the spleen, liver, and brain. The structures that were $tdTomato^+$ were confined in blood vessels marked by the expression of isolectin B4 (IB4) in the brain (Figure 3B, arrows), as well as in liver and spleen (Supplemental Figure 5A), suggesting that the $tdTomato^+$ cells were rbc trapped in vessels. Supporting this, these reporter-positive structures were negative for DAPI (data not shown). These results suggest rbc-specific expression of EpoR-Cre.

We first tested the effect on mice fed chow. Injections of CNO to chow-fed adult rbc-GsD mice had no discernible effects on EE, compared with saline injection (Figure 3C). Similarly, CNO had no significant effect on blood O_2 saturation, although there was a trend toward an increase in rbc-GsD mice (Figure 3D). We then tested the effects of rbc-Gs signaling under HFD conditions. After 2 weeks of HFD feeding, a single injection of CNO into rbc-GsD mice dramatically increased EE, compared with saline injections, whereas CNO had no effect in littermate controls that do not express GsD in rbc (Figure 3E). Interestingly, while CNO had no effect on blood O_2 content in controls, it significantly increased blood O_2 saturation in rbc-GsD mice (Figure 3F). Of note, CNO treatments led to no changes in locomotion of rbc-GsD animals (Supplemental Figure 5B) in either chow or HFD conditions, suggesting that the response in EE is not due to a change in activity. Notably, CNO treatment caused a significant reduction in the ratio

of glucose-6-phosphate(fructose-6-phosphate)/lactate (Figure 3G). Expectedly, as a result of increased glucose metabolism, ATP levels were also increased by CNO (Figure 3H). Thus, activation of Gs-cAMP signaling in rbc increases EE and blood O_2 content in mice fed HFD but not chow.

We then fed adult rbc-GsD mice HFD for 8 weeks to induce obesity. The obese GsD and littermate control mice were then continuously fed HFD and received daily CNO for another 2 weeks. Interestingly, while saline had no effects on EE, CNO immediately increases EE in rbc-GsD mice (Figure 4, A and B). Surprisingly, 2-week CNO treatment caused no significant changes in body weight, although there was a trend toward a greater reduction in body weight compared with their control mice (Figure 4C). Notably, chronic CNO treatment gradually stimulated food intake in rbc-GsD mice and became significant after 4 days of CNO injections (Figure 4D), suggesting that the increased feeding may be due to a compensatory response to CNO-induced EE stimulation.

Activation of cAMP signaling in rbc reduced HFD-induced tissue hypoxia. We then tested the impact of rbc-GsD signaling on tissue hypoxia by examining tissue oxygenation. As expected, compared with chow mice (Figure 5A), the adipose tissues of saline-treated HFD-fed mice exhibited a higher level of hypoxia (Figure 5B), which was reversed in CNO-treated HFD-fed mice (Figure 5C). In line with this, the expression of *Hif1α* mRNA, known to be induced by hypoxia, was higher in HFD-fed mice compared with chow fed mice. *Hif1α* expression was also reversed by CNO treatment in the HFD-fed rbc-GsD mice (Figure 5D). Importantly, chronic CNO treatment in rbc-GsD mice led to no significant changes in rbc number (Supplemental Figure 6A) or Hb levels (Supplemental Figure 6B), but it led to a dramatic reversal of white blood cell (Figure 5E) and eosinophil accumulation (Figure 5F) in response to HFD. Given the known correlation between inflammation and hypoxia (15, 18), the reduction in circulating leukocyte numbers is consistent with the improved tissue oxygenation triggered by CNO-GsD signaling in rbc. These findings indicate that activation of Gs-cAMP signaling in rbc is sufficient to reverse HFD-induced hypoxia independent of obesity.

Discussion

The current obesity epidemic is correlated with the availability of HFD, suggesting DIO as a major drive of obesity. Thus, insights on defective responses to HFD are essential to identify effective therapeutic targets against obesity. Prevalent studies in this direction mainly focus on nutrient surplus or partitioning in key metabolic tissues (1, 5, 6). Our data showed that HFD feeding increased cAMP, glycolysis, and ATP in rbc; raised blood O_2 level; and increased diet-induced EE, revealing — to our knowledge — a novel mechanism involving SNS→ rbc→ O_2 supply as part of the pathway underlying HFD-induced EE. These results establish that rbc-mediated blood O_2 supply plays an active role in augmenting diet-induced EE, thereby reducing susceptibility to DIO. This new finding provides an insight that blood O_2 supply actively participates in DIO, which is fundamentally distinct from the conventional view that tissue hypoxia is secondary to obesity (15, 18). We also identified rbc β-AR expression as a direct downstream target of HFD-activated SNS, raising an interesting possibility to use rbc as a therapeutic target for obesity prevention and treatment. It is conceivable that the same pathway may also operate in other conditions that demand higher levels of metabolism, such as exercise (31).

Defective HFD-induced EE is one major cause for DIO; however, how HFD affects EE remains unclear. Although acute HFD is known to increase EE (10, 18, 32, 33), the effect of long-term HFD remains controversial (34) but is thought to reduce EE (35, 36). Our results demonstrated that long-term HFD rather increased EE, which was accompanied by increased O_2 content. Notably, we compared EE between mice during the transition HFD feeding with comparable body weight, eliminating potential secondary effects of obesity, which is known to complicate analysis of EE comparison (37). Supporting its role in increasing EE, long-term HFD induces sustained SNS and mitochondrial activities (38, 39). Interestingly, on a chow diet, activation of Gs-cAMP signaling in rbc induced a trend for an increase in blood O_2 level but had no effects on EE. This result suggests that increasing O_2 availability alone is not sufficient to increase EE. SNS activation by HFD increased both blood O_2 level and a demand for a higher level of mitochondrial activities in metabolic tissues, through β-ARs in rbc and metabolic tissues, respectively. The selective effect of activation of rbc-Gs–cAMP in increasing EE on HFD but not chow suggests that SNS-induced EE by HFD is limited by O_2 availability and can be augmented by increased O_2 availability. Collectively, our results support a model that HFD activation of SNS engages both rbc and metabolic tissues, and initiates a coordinated response to promote diet-induced EE. A defective response to HFD in rbc to provide sufficient

O_2 supply leads to tissue hypoxia and, therefore, comprises diet-induced EE (i.e., increased but not to a sufficient extent to offset the increased energy intake associated with HFD), leading to DIO (Figure 5G).

Despite the established role for macrophages in EE (40, 41), it is unlikely that those cells contribute to reduced DIO in K→W mice in which β-ARs were lost in all blood cells. Macrophages rely on IL4 activation and release catecholamines to local fat tissues and in our in K→W mice, and β-ARs remained intact in fat tissues in our K→W mice. In addition, IL4 appears to have a major effect on cold tolerance but not diet induced obesity (40). HFD is not associated with IL4 changes (42), ruling out potential involvement of an IL4-mediated pathway in HFD-induced EE. Notably, a new study suggests a minimal role for macrophages in HFD-induced EE. Finally, our data on specific activation of Gs signaling in rbc, but not in any other blood cells, increases diet-induced EE. This was associated with reduced immune cells including eosinophil cells, strongly arguing against a role for macrophage involvement in increasing HFD-induced EE.

Our data on rbc metabolites suggest a pathway comprising HFD-induced activation of SNS → β-ARs → Gs-cAMP signaling → increased glycolysis→ increased ATP. Although the exact mechanism underlying the improved blood O_2 supply remains unknown, the increased ATP levels may contribute significantly. Rbc ATP release increases vasodilation (43–45), which may increase O_2 loading in the lung and unloading in metabolic tissues (44–46). Notably, activation of β-ARs in rbc improves membrane deformation (43, 47, 48) and therefore increases infiltration of rbc within metabolic tissues. Neither 2,3-DPG nor P50 were significantly altered by deficiency of β-ARs or HFD, suggesting that HFD-induced increases in O_2 availability do not involve changes in O_2-Hb affinity.

Activation of rbc-Gs–cAMP signaling greatly reduced hypoxia, which was not due to reduced usage of O_2 because Gs-cAMP signaling instead increases diet-induced EE. Thus, the reversal of hypoxia was caused by increased blood O_2 availability. Consistent with reduced hypoxia, activation of rbc-Gs signaling reversed DIO-induced increases in WBCs and eosinophil, which are known to be associated with inflammation and tissue hypoxia (15). These results suggest a role for SNS activation of rbc in alleviating HFD-induced tissue hypoxia. Thus, meeting the demand for more O_2 in metabolic tissues during DIO is an effective strategy to improve metabolic dysfunctions associated with DIO.

In summary, we identified a previously unappreciated role for β-ARs in rbc in mediating SNS action on HFD-induced EE by meeting the demand for more O_2 availability during HFD and reducing hypoxia. Given the current obesity epidemic and lack of effective treatment choices against obesity complications, our findings provide potential alternative strategies to reduce DIO by activating diet-induced EE through increasing rbc O_2 delivery.

Methods

Animal care. Mice were housed at 21°C–22°C with a 12-hour light/12-hour dark cycle with water and food provided ad libitum, standard mouse chow (Teklad F6 Rodent Diet 8664; 4.05 kcal/g, 3.3 kcal/g metabolizable energy, 12.5% kcal from fat; Harlan Teklad) or HFD (D12331, Research Diets). C57BL/6J and FVB mice were purchased from The Jackson Laboratory, and breeding pairs were maintained to generate study subjects. Mice lacking all 3 β-ARs (β-less) were on FVB background and provided by Bradford Lowell of Harvard Medical School (Boston, Massachusetts, USA) (13). Conditional Gs-DREADD mice (27) and EpoR-Cre mice (28, 29) were obtained from Rebecca Berdeaux and Yang Xia of the University of Texas Medical School at Houston. The mice were crossed to generate rbc-GsD. All mice used were heterozygous for Gs-DREADD. All study subjects are littermates. To validate EpoR-Cre expression, EpoR-Cre mice were crossed with Ai9 mice (The Jackson Laboratory) to generate EpoR-Cre::Ai9 mice, in which Cre expression can be directly visualized by tdTomato, a variant red fluorescence protein (RFP), under fluorescent microscopes (30). Female mice are known to develop limited obesity in response to HFD and exhibit estrous cycles, which may produce profound changes in O_2 content. Thus, this study primarily focused on males.

BMT. BMT experiments were performed as previously described (49). Briefly, BM cells were harvested from male WT and β-less donor mice by gently flushing their femurs using syringe (26 G needle) with RPMI 1640 medium (GIBCO). After purification, rbc were removed using the rbc lysis buffer (150 mM NH_4Cl, 10 mM $KHCO_3$, 0.1 mM EDTA). Cells were centrifuged and resuspended in Dulbecco's Phosphate Buffered Saline (DPBS, HyClone, SH30028.02). BM cells were counted and prepared in the concentration of 25 × 10^6cells/ml in DPBS. WT recipient mice were then lethally irradiated (950 rad) and immediately injected with either WT (W→W, K→W) or β-less (K→K) donor cells (5 × 10^6 cells in

0.2 ml) through tail vein injections. Mice were single housed and recovered for 4 weeks to reconstitute BM of donors. Then, they were switched to HFD and maintained on HFD for 5 weeks. Food intake and body weight were monitored weekly.

Metabolic rate by CLAMS. O_2 consumption, CO_2 production, RER or locomotor activity levels were measured using indirect calorimetry. Mice at the age of 8–18 weeks old were individually housed at room temperature (21°C–22°C) in chambers of a Comprehensive Lab Animal Monitoring System (CLAMS, Columbus Instruments). Food and water were provided ad libitum. Mice were acclimatized in the chambers for at least 2 days prior to data collection. For Iso effects on EE, groups of control FVB and β-less male mice with comparable age and body weight were placed in the chamber. On day 3, both groups of mice received a single s.c. injection of saline at 12:00 hours, and on the following day (day 4), they received Iso (1 mg/kg, body weight [bw]) at the same time when they received saline injections on the previous day. O_2 consumption was monitored for the ensuing 3 hours and averaged. The averaged O_2 consumption levels were compared between saline and Iso treatments in each genotype. For the studies for the correlation between O_2 consumption and blood O_2 contents during day and night periods, after 2 days of acclimation time, mice were measured for O_2 consumption for 24 hours. Low and high levels of O_2 consumption were observed at ZT5–ZT6 and ZT12–ZT13, respectively. For BMT groups, after a period of 4 weeks allowed for full blood reconstitution, they were on HFD feeding for at least 5 weeks. EE was measured using CLAMS as described above. For the rbc-Gs signaling study group, rbc-GsD mice and their control mice were fed HFD for 8 weeks to develop DIO. Mice were placed to CLAMS chambers as described above. They received daily i.p. CNO (Tocris Bioscience, 1 mg/kg, bw).

Blood O_2 level measurements. Samples of mixed arterial and vein blood were collected from tails using a capillary collection device (ITC International) as previously reported (50). Blood samples were transferred to cuvettes (ITC International) immediately, and the levels of O_2 contents, O_2-Hb, and total Hb were measured using whole blood oximeter (Avoximeter 1000E, ITC International). O_2-Hb indicates the percent of O_2 binding to total Hb. Non–O_2-Hb levels were derived based on actual measurement of O_2-Hb levels. A volume of 50 μl blood was sufficient for each measurement. For measurements in control and β-less mice, each genotype (8–10 weeks of age) was divided into two groups, and each received either a single s.c. of saline or Iso (1 mg/kg, bw). Blood samples were collected 3.5 hours after injections. Food was removed during the testing period to avoid potential confounding effects from feeding. For the measurement in day and night periods, male FVB at the age of 8–10 weeks old with food ad libitum were sampled twice for tail blood at light (ZT5–ZT6) and night (ZT12–ZT13) period. For BMT mice, O_2 content, O_2-Hb, and total Hb were measured 1 week before BMT and after 5 weeks of feeding on HFD after BMT. For the rbc activation study, O_2 content, O_2-Hb, and total Hb were measured on chow from rbc-GsD and their control group. After 2 weeks of HFD, both groups of mice received saline or i.p. CNO (1 mg/kg, bw), and 50 minutes later, blood O_2 contents were measured as described above.

Correlation between blood O_2 levels and body weight. Age-matched C57BL/6J male mice (9–10 weeks old) were measured for body weight, O_2 content, and average food intake over 4 days. Potential correlations between O_2 content and body weight or food intake were analyzed using Pearson's correlation tests. A separate cohort of the same mice were used and switched to HFD (D12331, Research Diets, 58 kcal% fat w/sucrose) and maintained on HFD for 8 weeks. Body weight, food intake, and O_2 content were measured before and 8 weeks after the switch to HFD.

Chemical assays. Tail blood samples were collected in heparinized tubes from BMT mice fed with HFD for at least 5 weeks and stored at –80°C until erythrocyte ATP and cAMP measurements were made. Briefly, for rbc ATP, 10 μl rbc was added to 190μl 0.6 M cold perchloric acid on ice, vortexed, and centrifuged at 20,000 *g* for 10 minutes at 4°C. Supernatant (100 μl) was transferred to a new tube and neutralized with 25 μl 0.6 M $KHCO_3$/0.72 M KOH. Finally, the sample was centrifuged at 20,000 *g* for 5 minutes, and the supernatant was subjected to bioluminescence assay (Sigma-Aldrich, FL-AA). For 2,3-DPG measurement, 10 μl rbc were added to 50 μl 0.6 M cold perchloric acid on ice, vortexed, and centrifuged at 20,000 *g* for 10 minutes at 4°C. Supernatant (40 μl) was transferred to a new tube and neutralized with 5 μl 2.5 M K_2CO_3. Finally, the sample was centrifuged at 20,000 *g* for 10 minutes, and the supernatant was subjected to 2,3-BPG assay (Roche Diagnostics). For cAMP measurement using ELISA kits, rbc were lysed and centrifuged at 15,000 *g* for 10 minutes at 4°C. Supernatant was transferred to a new tube and followed manufacturer instruction of commercial ELISA kit (Enzo Life Sciences,ADI-900-163). The values were normalized to total protein concentration. For rbc cAMP and ATP levels in FVB WT and β-less mice — along with

lactate and glucose-6-phosphate(fructose-6-phophate)/lactate levels in rbc-GsD mice — tail blood was collected in a heparinated tube 50 minutes after i.p. injection of CNO (1 mg/kg/bw) or saline both rbc-GsD and their littermate controls. Cells were counted after washing 3 times with 1× PBS through cycle of centrifugation-resuspension. Rbc were harvested at 5.6×10^6 cells per individual sample and kept in a –80ºC freezer until metabolomics analysis.

For the metabolomics analysis, rbc number at 5.6×10^6 cells per sample was used, and the concentrations of ATP, cAMP, glucose-(fructose-)6-phosphate, and 2,3-DGP were determined by the Metabolomics Core at Baylor College of Medicine by Feng Li as described previously (51).

IHC. Blood was collected from a tail in heparinated tube and incubated with DAPI (PN 320858, RNAscope Reagent kit, Advanced Cell Diagnostics) for 1 minute. The samples were observed and images were taken using a Nikon Eclipse TE2000E Widefield Fluorescence Microscope.

Brain, liver, and spleen tissues of EpoR-Cre mice crossed with Ai9 mice were collected after cardiac perfusion with 4% paraformaldehyde. After overnight postfixation, sections were made using cryostat (Leica, CM1850). The liver and spleen sections were processed for antigen retrieval, followed by incubation with 0.3% Tween 20 for 30 minutes. All sections of brain, liver, and spleen were incubated with Sea blocking buffer (Thermo Fisher Scientific, 37527) for 30 minutes followed by blocking with streptavidin (Vector Laboratories, SP-2002) and biotin for 30 minutes, respectively. Griffonia simplicifolia lectin 1 IB4 (GSL1-IB4) was diluted at 1:100 concentration and used for the sections overnight at 4ºC. After being rinsed 3× with 1× PBS, sections were visualized with Alexa Fluor 488 streptavidin (Thermo Fisher Scientific, S32354) diluted at a 1:200 concentration. The signal was captured and imaged using Nikon Eclipse TE2000E Widefield Fluorescence Microscope.

Rbc-GsD mice and their littermate control mice were on HFD for 8 weeks. When they developed DIO, both groups of mice were on daily i.p. injection of CNO (1 mg/kg, bw, 10:00 and 17:00 for 2 weeks. Mice were received pimonidazole (hypoxyprobe-1, 80mg/kg, bw; Chemicon International, HP2-100), and 45 minutes later, s.c. adipose tissues were collected for immunostaining. Tissues were fixed in 10% normal formalin buffer, processed, and then paraffin embedded. Deparaffinized sections were incubated with 10% of BSA for 1 hour, followed by incubation with anti-pimonidazole conjugated with FITC (monoclonal, 1:100) for 1 hour. After being rinsed 3× with 1× PBS, sections were further incubated with anti–FITC-HRP (Chemicon International, catalog HP2-100) (1:00) for 1 hour to amplify signals. The staining was visualized using DAB system (Vector Laboratories, SK-4105) and then counterstained with hematoxylin. Images were obtained using upright Axiocam 506 color camera (Zeiss Axio Scope).

mRNA quantification by quantitative PCR (qPCR). s.c. adipose tissues were quickly collected and frozen. Total RNA was isolated using Trizol (Invitrogen) and RNeasy Mini kit (QIAGEN) by following company instruction. After qualifying and quantifying the total RNA using NanoDrop 2000 Spectrophotometer (Thermo Fisher Scientific), cDNA was prepared with 1 μg of the RNA. qPCR was performed using CFX96 Real-Rime System (Bio-Rad). The following primer sequences were used for the assessment of gene expression levels: HIF1-α (forward, 5′ - ACCTTCATCGGAAACTCCAAAG - 3′; reverse, 5′ - ACTGTTAGGCTCAGGTGAACT - 3′) and GAPDH as internal control (forward, 5′ - AGGTCGGTGTGAACGGATTTG - 3′; reverse, 5′ - TGTAGACCATGTAGTTGAGGTCA - 3′). Data were analyzed using ΔΔCt method, and the mRNA expression levels between groups were compared in fold changes.

Statistics. Data represent means ± SEM. Statistical analysis was performed using GraphPad Prism. Statistical significance among the groups was tested using 2-tailed Student's *t* test or ANOVA tests. Correlation was analyzed by Pearson correlation coefficient. Statistical significance was defined as $P < 0.05$.

Study approval. Animal care and procedures were approved by the University of Texas Health Science Center at Houston IACUC.

Author contributions

ERK and QT conceived the study. ERK performed the majority of the study with essential help from SF, Yuangzhong X., and LRM. HL, YZ, and YC contributed to the BMT studies. WO, Kaiqi S., CCL, and Y. Xia contributed to the biochemical measurements of rbc. FL provided metabolomics measurements on rbc. DA, Kai S., Yong X., and RB provided essential reagents for the studies. ERK and QT wrote the manuscript with essential inputs from all authors. QT is the guarantor of this work and, as such, had full access to all the data in the study and takes responsibility for the integrity of the data and the accuracy of the data analysis.

Acknowledgments

We thank Bruce Toben from ITC for help on the blood O_2 measurement device. This work was supported by NIH R01DK092605, UT BRAIN Initiative, CTSA UL1 TR000371, Welch Foundation (L-AU0002), Grand-in-aid from American Heart Association (15GRNT22370024), and Basic Research Award (1-15-BS-184) from American Diabetes Association (all to QT); NIH 5F31DA041703-02 to LM; NIH R01DK093587 and R01DK101379 to Yong X.; NIH R01-AR059847 and R01-DK092590 to RB; the American Heart Association (15POST25090134) to DA; and NIH (HL119549, DK083559, and HL113574) to Y.Xia. This work was also supported by CPRIT RP120092 Proteomic and Metabolomic Core Facility, NCI/ 2P30CA125123-09 Shared Resources Metabolomics Core, funds from Dan L. Duncan Cancer Center (DLDCC) of Baylor college of Medicine, and funds from Alkek Center for Molecular Discovery, Metabolomic Core Facility to FL. QT is the holder of Cullen Chair in Molecular Medicine at McGovern Medical School.

Address correspondence to: Qingchun Tong, Brown Foundation Institute of Molecular Medicine, 1825 Pressler Street, SRB430G, Houston, Texas 77030, USA. Phone: 713.500.3453;Email: qingchun.tong@uth.tmc.edu.

1. Ryan KK, Woods SC, Seeley RJ. Central nervous system mechanisms linking the consumption of palatable high-fat diets to the defense of greater adiposity. *Cell Metab*. 2012;15(2):137–149.
2. Heitmann BL, et al. Obesity: lessons from evolution and the environment. *Obes Rev*. 2012;13(10):910–922.
3. Temelkova-Kurktschiev T, Stefanov T. Lifestyle and genetics in obesity and type 2 diabetes. *Exp Clin Endocrinol Diabetes*. 2012;120(1):1–6.
4. Tseng YH, Cypess AM, Kahn CR. Cellular bioenergetics as a target for obesity therapy. *Nat Rev Drug Discov*. 2010;9(6):465–482.
5. Cannon B, Nedergaard J. Nonshivering thermogenesis and its adequate measurement in metabolic studies. *J Exp Biol*. 2011;214(Pt 2):242–253.
6. Müller MJ, Bosy-Westphal A. Adaptive thermogenesis with weight loss in humans. *Obesity (Silver Spring)*. 2013;21(2):218–228.
7. Wijers SL, Saris WH, van Marken Lichtenbelt WD. Recent advances in adaptive thermogenesis: potential implications for the treatment of obesity. *Obes Rev*. 2009;10(2):218–226.
8. Trayhurn P. Hypoxia and adipocyte physiology: implications for adipose tissue dysfunction in obesity. *Annu Rev Nutr*. 2014;34:207–236.
9. Shimizu I, et al. Vascular rarefaction mediates whitening of brown fat in obesity. *J Clin Invest*. 2014;124(5):2099–2112.
10. Morrison SF, Madden CJ, Tupone D. Central neural regulation of brown adipose tissue thermogenesis and energy expenditure. *Cell Metab*. 2014;19(5):741–756.
11. Lowell BB, Bachman ES. Beta-Adrenergic receptors, diet-induced thermogenesis, and obesity. *J Biol Chem*. 2003;278(32):29385–29388.
12. Robidoux J, Martin TL, Collins S. Beta-adrenergic receptors and regulation of energy expenditure: a family affair. *Annu Rev Pharmacol Toxicol*. 2004;44:297–323.
13. Bachman ES, et al. betaAR signaling required for diet-induced thermogenesis and obesity resistance. *Science*. 2002;297(5582):843–845.
14. Wood IS, de Heredia FP, Wang B, Trayhurn P. Cellular hypoxia and adipose tissue dysfunction in obesity. *Proc Nutr Soc*. 2009;68(4):370–377.
15. Ye J. Emerging role of adipose tissue hypoxia in obesity and insulin resistance. *Int J Obes (Lond)*. 2009;33(1):54–66.
16. Quintero P, Milagro FI, Campión J, Martínez JA. Impact of oxygen availability on body weight management. *Med Hypotheses*. 2010;74(5):901–907.
17. Gupte AA, et al. High-fat feeding-induced hyperinsulinemia increases cardiac glucose uptake and mitochondrial function despite peripheral insulin resistance. *Endocrinology*. 2013;154(8):2650–2662.
18. Lee YS, et al. Increased adipocyte O2 consumption triggers HIF-1α, causing inflammation and insulin resistance in obesity. *Cell*. 2014;157(6):1339–1352.
19. Hosogai N, et al. Adipose tissue hypoxia in obesity and its impact on adipocytokine dysregulation. *Diabetes*. 2007;56(4):901–911.
20. Ye J, Gao Z, Yin J, He Q. Hypoxia is a potential risk factor for chronic inflammation and adiponectin reduction in adipose tissue of ob/ob and dietary obese mice. *Am J Physiol Endocrinol Metab*. 2007;293(4):E1118–E1128.
21. Harrison T, et al. Erythrocyte G protein-coupled receptor signaling in malarial infection. *Science*. 2003;301(5640):1734–1736.
22. Lynch PJ. Cutis marmorata telangiectatica congenita associated with congenital glaucoma. *J Am Acad Dermatol*. 1990;22(5 Pt 1):857.
23. Oishi K, et al. Clock mutation affects circadian regulation of circulating blood cells. *J Circadian Rhythms*. 2006;4:13.
24. Enriori PJ, et al. Diet-induced obesity causes severe but reversible leptin resistance in arcuate melanocortin neurons. *Cell Metab*. 2007;5(3):181–194.
25. Bernstein D. Cardiovascular and metabolic alterations in mice lacking beta1- and beta2-adrenergic receptors. *Trends Cardiovasc Med*. 2002;12(7):287–294.
26. Wess J, Nakajima K, Jain S. Novel designer receptors to probe GPCR signaling and physiology. *Trends Pharmacol Sci*. 2013;34(7):385–392.
27. Akhmedov D, Mendoza-Rodriguez MG, Rajendran K, Rossi M, Wess J, Berdeaux R. Gs-DREADD Knock-In Mice for Tissue-Specific, Temporal Stimulation of Cyclic AMP Signaling. *Mol Cell Biol*. 2017;37(9):e00584-16.
28. Liu H, et al. Beneficial Role of Erythrocyte Adenosine A2B Receptor-Mediated AMP-Activated Protein Kinase Activation in High-Altitude Hypoxia. *Circulation*. 2016;134(5):405–421.

29. Heinrich AC, Pelanda R, Klingmüller U. A mouse model for visualization and conditional mutations in the erythroid lineage. *Blood*. 2004;104(3):659–666.
30. Madisen L, et al. A robust and high-throughput Cre reporting and characterization system for the whole mouse brain. *Nat Neurosci*. 2010;13(1):133–140.
31. Morris EM, et al. Aerobic capacity and hepatic mitochondrial lipid oxidation alters susceptibility for chronic high-fat diet-induced hepatic steatosis. *Am J Physiol Endocrinol Metab*. 2016;311(4):E749–E760.
32. Tong Q, Ye CP, Jones JE, Elmquist JK, Lowell BB. Synaptic release of GABA by AgRP neurons is required for normal regulation of energy balance. *Nat Neurosci*. 2008;11(9):998–1000.
33. Lorenzen J, Frederiksen R, Hoppe C, Hvid R, Astrup A. The effect of milk proteins on appetite regulation and diet-induced thermogenesis. *Eur J Clin Nutr*. 2012;66(5):622–627.
34. Carneiro IP, et al. Is Obesity Associated with Altered Energy Expenditure? *Adv Nutr*. 2016;7(3):476–487.
35. Choi MS, Kim YJ, Kwon EY, Ryoo JY, Kim SR, Jung UJ. High-fat diet decreases energy expenditure and expression of genes controlling lipid metabolism, mitochondrial function and skeletal system development in the adipose tissue, along with increased expression of extracellular matrix remodelling- and inflammation-related genes. *Br J Nutr*. 2015;113(6):867–877.
36. Ravussin E, et al. Reduced rate of energy expenditure as a risk factor for body-weight gain. *N Engl J Med*. 1988;318(8):467–472.
37. Tschöp MH, et al. A guide to analysis of mouse energy metabolism. *Nat Methods*. 2011;9(1):57–63.
38. Morgan DA, Thedens DR, Weiss R, Rahmouni K. Mechanisms mediating renal sympathetic activation to leptin in obesity. *Am J Physiol Regul Integr Comp Physiol*. 2008;295(6):R1730–R1736.
39. Montgomery MK, et al. Mouse strain-dependent variation in obesity and glucose homeostasis in response to high-fat feeding. *Diabetologia*. 2013;56(5):1129–1139.
40. Qiu Y, et al. Eosinophils and type 2 cytokine signaling in macrophages orchestrate development of functional beige fat. *Cell*. 2014;157(6):1292–1308.
41. Nguyen KD, et al. Alternatively activated macrophages produce catecholamines to sustain adaptive thermogenesis. *Nature*. 2011;480(7375):104–108.
42. Miyazaki Y, et al. Effect of high fat diet on NKT cell function and NKT cell-mediated regulation of Th1 responses. *Scand J Immunol*. 2008;67(3):230–237.
43. Sprague RS, Ellsworth ML, Stephenson AH, Lonigro AJ. Participation of cAMP in a signal-transduction pathway relating erythrocyte deformation to ATP release. *Am J Physiol, Cell Physiol*. 2001;281(4):C1158–C1164.
44. Sprague RS, Stephenson AH, Ellsworth ML, Keller C, Lonigro AJ. Impaired release of ATP from red blood cells of humans with primary pulmonary hypertension. *Exp Biol Med (Maywood)*. 2001;226(5):434–439.
45. Jensen FB. The dual roles of red blood cells in tissue oxygen delivery: oxygen carriers and regulators of local blood flow. *J Exp Biol*. 2009;212(Pt 21):3387–3393.
46. Kunert MP, Liard JF, Abraham DJ, Lombard JH. Low-affinity hemoglobin increases tissue PO2 and decreases arteriolar diameter and flow in the rat cremaster muscle. *Microvasc Res*. 1996;52(1):58–68.
47. Tuvia S, Moses A, Gulayev N, Levin S, Korenstein R. Beta-adrenergic agonists regulate cell membrane fluctuations of human erythrocytes. *J Physiol (Lond)*. 1999;516 (Pt 3):781–792.
48. Muravyov AV, Tikhomirova IA, Maimistova AA, Bulaeva SV. Extra- and intracellular signaling pathways under red blood cell aggregation and deformability changes. *Clin Hemorheol Microcirc*. 2009;43(3):223–232.
49. Lim H, et al. Negative regulation of pulmonary Th17 responses by C3a anaphylatoxin during allergic inflammation in mice. *PLoS One*. 2012;7(12):e52666.
50. Xu Y, et al. Profound and rapid reduction in body temperature induced by the melanocortin receptor agonists. *Biochem Biophys Res Commun*. 2014;451(2):184–189.
51. Liu X, Lu YF, Guan X, Zhao M, Wang J, Li F. Characterizing novel metabolic pathways of melatonin receptor agonist agomelatine using metabolomic approaches. *Biochem Pharmacol*. 2016;109:70–82.